

Vesicle formation induced by thermal fluctuations

Andreu F. Gallen¹, J. Roberto Romero-Arias², Rafael A. Barrio³, and Aurora Hernandez-Machado^{1,4}

Received Date

Accepted Date

DOI: 00.0000/xxxxxxxxxx

The process of fission and vesicle formation depends on the geometry of the membrane that will split. For instance, a flat surface finds it difficult to form vesicles because of the lack of curved regions where to start the process. Here we show that vesicle formation can be promoted by temperature, by using a membrane phase field model with Gaussian curvature. We find a phase transition between fluctuating and vesiculation phases that depends on temperature, spontaneous curvature, and the ratio between bending and Gaussian moduli. We analysed the energy dynamical behaviour of these processes and found that the main driving ingredient is the Gaussian energy term, although the curvature energy term usually helps with the process as well. We also found that the chemical potential can be used to investigate the temperature of the system. Finally we address how temperature changes the condition for spontaneous vesiculation for all geometries, making it happen in a wider range of values of the Gaussian modulus.

1 Introduction

Lipid vesicles, also known as liposomes or simply vesicles, are structures that are crucial for many biological processes, as transport vesicles¹, secretory vesicles², and endocytosis³. Many of these biological systems require to create and destroy vesicles constantly, e.g. the Golgi apparatus^{4,5}, the synaptic system^{6,7}, or enveloped viruses^{8,9}. Even red blood cells are known to lose membrane when they become old through shedding of microvesicles and leading to a change of their surface-volume ratio¹⁰. Thus, there is great interest in gaining insight on the dynamics of vesicle formation, also referred to as vesiculation. Vesicles are also produced artificially, either from preformed bilayers or by building them directly from an organic mixture of lipids in contact with an aqueous medium¹¹, using some electroformation¹² or thin-film hydration methods¹³.

In a previous article¹⁴, the vesiculation of a membrane tube was studied by introducing the Gaussian curvature energy term. This Gaussian term is necessary to study topological transitions on membranes and has usually been neglected¹⁵. The membrane tube geometry helped the fission process and leads to the membrane splitting into multiple vesicles¹⁴. However, there are some membrane geometries that instead of helping vesicle formation process they hinder it like, for example, a perfectly flat membrane.

A perfectly flat membrane is a geometry that hinders this budding process as it lacks any curved region. Without any point more curved than the other, even if budding is energetically favourable there is no preferred point from where to start the membrane budding process. This, in turn, stops vesicula-

tion, even in the case where generating vesicles is energetically favourable. However, in nature vesiculation happens in wide variety of situations and with plenty of membrane geometries for the initial membrane. It is known that vesicle formation is a temperature-dependent process^{3,16} and that temperature gradients affect the phase behaviour heterogeneous membranes¹⁷ and can change the lipid phase between fluid and gel states¹⁸. In experimental works, it has been shown that the size of the vesicles depend on preparation methods, the type of lipid used and the temperature¹⁹ and even the temperature has been used to produce fission of vesicles in Giant Unilamellar Vesicles (GUVs)²⁰ considering the first order phase transition between the gel and fluid states in the lipids. In live organisms we also have temperature dependence many processes like synaptic signalling, endocytosis, and in vesicle trafficking²¹.

The processes beyond membrane fission has been challenging. There are some works in microscopic modelling with molecular dynamic simulations²²⁻²⁴, but in the mesoscopic modelling scales little has been done, and there is a bit understanding on topological transitions^{25,26}. In mesoscopic models, one needs to consider the energy of the membrane as a continuous surface, instead of going molecule by molecule. Thus, in this work, we study some mechanisms that promote –or even induce– the formation of a vesicle from a non-favourable geometry.

To promote the vesiculation from a completely flat membrane, one introduces the effect of finite temperatures to the previously mentioned model¹⁴. We develop a three dimensional model to study the dynamics of spontaneous vesicle formation from a flat membrane by adding a thermal noise. This model will be accurate for vesicles or regions of a membrane where there are no proteins present. With these considerations, one shall expect to deform the membrane enough and start the vesiculation process. However, it is not as simple as that, as there is an energy barrier that is impeding the flat membrane to change shape and form buds. Thus, we assemble a phase diagram between fluctuation and vesiculation states and we find that the topological stability

¹Departament Física de la Matèria Condensada, Universitat de Barcelona, E-08028 Barcelona, Spain.

²Instituto de Investigaciones en Matemáticas Aplicadas y en Sistemas, Universidad Nacional Autónoma de México, 01000 Ciudad de México, Mexico.

³Instituto de Física, U.N.A.M., 01000, Ap. Postal 101000, México D.F., México

⁴Institute of Nanoscience and Nanotechnology (IN2UB), 08028 Barcelona, Spain

of the membrane depends on the bending and Gaussian moduli, the spontaneous curvature and the temperature of the system. Also, we find that temperature is only needed to trigger the process but that when one has a curved enough region the vesiculation process will go on, even when turning the temperature back to zero. Surprisingly, we see no topological transitions for positive Gaussian modulus. One would expect the membrane to form tunnels and channels but the topology of the system remains unchanged even for excessively large temperatures.

2 Model

The model follows the Canham-Helfrich free energy and its phase-field approaches used for fission of membrane tubes¹⁴. The Canham-Helfrich free energy is written as

$$F = \int_A \left(\frac{\bar{\kappa}}{2} (C - c_0)^2 + \bar{\kappa}_G K + \gamma_A \right) dA + \int_V \Delta p dV, \quad (1)$$

where $\bar{\kappa}$ and $\bar{\kappa}_G$ are the bending and Gaussian moduli, respectively. C is the total curvature, c_0 is the spontaneous curvature and K is the Gaussian curvature. The parameters γ_A and Δp are Lagrange multipliers that ensure the conservation of the area and the volume respectively. These last can be understood as an effective surface tension and an osmotic pressure that works against changes of area and volume, respectively.

Usually, by using the Gauss-Bonnet theorem one can avoid the Gaussian curvature contribution to the energy, but in this work, we consider the Gaussian contribution since we are interested in studying the formation of vesicles. The Gauss-Bonnet theorem states that the integral of the Gaussian curvature over a surface is proportional to the surface Euler characteristic $\chi(\Omega)$, which is a topological invariant²⁷. The Euler characteristic describes the system by the number of holes g and objects N like $\chi(\Omega) = 2(N - g)$. In general, one can describe a system that increases the number of objects and generate vesicles with $\bar{\kappa}_G < 0$ and a system that increases the number of holes when $\bar{\kappa}_G > 0$ ²⁵.

From the free energy of equation (1), one can compute the minimum energy necessary to form a spherical vesicle from a planar membrane. The energy required, if we neglect the bilayer thickness effect¹¹, reads

$$f = (2\bar{\kappa} + \bar{\kappa}_G) \frac{A}{R^2}, \quad (2)$$

where R is the radius of the vesicle, A is its area. To have vesicles generated spontaneously, we need this energy contribution to be negative. Thus, one can obtain that for the vesicle formation to be spontaneous, one requires $-\bar{\kappa}_G > 2\bar{\kappa}$. Therefore, one should find spontaneous vesiculation depending on the values of $\bar{\kappa}_G$ and $\bar{\kappa}$. The values of the bending modulus are estimated from elastic properties of the membranes²⁵. However, the Gaussian modulus needs an indirect technique for measurement. An experimental²⁸ and theoretical²⁹ value of Gaussian modulus is estimated as $\bar{\kappa}_G \approx -15K_B T$. In a previous work¹⁴, we studied a phase diagram on vesicle formation and we found three possible stable states that corresponds to: i) membrane fission when the negative Gaussian modulus $\bar{\kappa}_G$ is much larger than the bending

modulus $\bar{\kappa}$; ii) no fission membrane when $\bar{\kappa}_G$ is negative but not much larger than $\bar{\kappa}$; and iii) multiple self-connected membrane for positive $\bar{\kappa}_G$ in which many holes are developed in a single continuous membrane.

In the phase diagram $(\bar{\kappa}_G, \bar{\kappa})$, one finds that for negative Gaussian modulus there is a transition between spontaneous vesiculation state and a topologically stable state defined by the line $\bar{\kappa}_G = -2\bar{\kappa}$. As one can compute the energy cost to generate a vesicle, one may compute the energy cost necessary when one has a Gaussian modulus that does not comply to that condition. Thus, in order to generate a spherical vesicle of area $A = 4\pi R^2$ with radius R and $\bar{\kappa}_G < 0$, the energy required is $f = 4\pi(2\bar{\kappa} - |\bar{\kappa}_G|)$. This energy ΔE is the minimum energy required for generating a vesicle. Introducing now a spontaneous curvature c_0 ³⁰, we get that the energy barrier is $\Delta E = 4\pi(2\bar{\kappa} + \bar{\kappa}_G)(1 - Rc_0)^2$. Fission is a thermally activated process with a characteristic time-scale of around $\tau = t_0 e^{\Delta E/K_B T}$ where t_0 is the typical time scale of a thermal fluctuation that depending on the system goes from $1ms$ in membrane tubes to $1ms$ on the Golgi apparatus^{31,32}.

Thus the system will follow an Arrhenius law. For long enough times, vesiculation will occur in any case that has a thermal energy $K_B T$ larger than ΔE . If T is too small the time required for vesiculation will be much longer than the simulation time. Therefore, depending on whether the thermal energy, $E_T = k_B T$, is bigger or smaller than this energy barrier, one obtains spontaneous vesicle formation or not. This is what will distinguish between the two phases that we study in this paper, the fluctuating and the vesiculating one.

Vesiculation is an irreversible process, as it increases the entropy of the system and we can ensure that for a time long enough the system will generate vesicles. Therefore, for a system with a temperature T the condition for spontaneous vesicle formation will be

$$-\bar{\kappa}_G > 2\bar{\kappa} - k_B T. \quad (3)$$

With this formulation, the membrane may exhibit spontaneous fission for new values of $\bar{\kappa}_G$ that could not vesiculate before.

Membrane phase field model

Phase field models are used in problems where tracking the position of an interface can be difficult or computationally costly. These models have been used to study membranes successfully in the past for both equilibrium and dynamic systems³³⁻³⁶. One can write the free energy of the membrane from equation (1) as a function of an order parameter ϕ and its derivatives³⁷. This order parameter ϕ will define if a given point in space corresponds to: the membrane, the inner, or the outer fluid of the vesicle. We can obtain the dynamic equation by performing the functional derivative of both contributions to the free energy and write the temporal evolution. The dynamic equation is a Ginzburg-Landau formalism (model B³⁸) for a conserved order parameter as

$$\frac{\partial \phi}{\partial t} = \nabla^2 \left(\frac{\delta F_{C_0}}{\delta \phi} + \frac{\delta F_K}{\delta \phi} \right), \quad (4)$$

in which the mean and spontaneous curvature F_{C_0} contribution

reads like³³

$$F_{C_0} = \kappa \int_{\Omega} \left((\phi - \varepsilon C_0)(\phi^2 - 1) - \varepsilon^2 \nabla^2 \phi \right)^2 dV, \quad (5)$$

where ε is the width of the interface, $\kappa = 3\bar{\kappa}/4\sqrt{2}\varepsilon^3$ and $C_0 = c_0/\sqrt{2}$. Similarly, the Gaussian contribution is¹⁴

$$F_K = \int \bar{\kappa}_G K dS = \bar{\kappa}_G \frac{3}{4\sqrt{2}\varepsilon} \int \sum_{i<j} \frac{(1-\phi^2)^2}{2} (Q_{ii}Q_{jj} - Q_{ij}^2) dV, \quad (6)$$

where Gaussian modulus $\kappa_G = 3\bar{\kappa}_G/(4\sqrt{2}\varepsilon)$ and Q_{ij} is curvature tensor (see Supporting Information for the exact expression). The dynamical equation (4) can be written explicitly in terms of the phase field order parameter ϕ as

$$\begin{aligned} \frac{\partial \phi}{\partial t} = & \kappa \nabla^2 \left((3\phi^2 - 1 - 2\phi\varepsilon C_0)\Phi - \varepsilon^2 \nabla^2 \Phi + \gamma_A \nabla^2 \phi \right) \\ & - \kappa_G \nabla^2 \left(\frac{12\phi}{1-\phi^2} T_1 + \frac{2(3\phi^2+1)}{(1-\phi^2)^2} T_2 \right), \end{aligned} \quad (7)$$

where $\Phi = (\phi - \varepsilon C_0)(\phi^2 - 1) - \varepsilon^2 \nabla^2 \phi$. The terms T_1 and T_2 , which can be found in the Supporting Information, are computed from various derivatives of ϕ ^{14,39}.

Even though in eq. (7) we still keep the Lagrange multiplier for area γ_A in this membrane geometry of an infinite flat surface we do not need to impose the conservation of surface area. The membrane will behave as if connected to an area reservoir and thus we will not introduce γ_A in this numerical implementation. Regarding the volume, local volume conservation is always ensured thanks to the diffusive behaviour of eq (7) as we have all the dynamics inside the Laplacian.

Numerical Implementation

The equation (7) is highly non-linear with the order parameter and therefore shall solve it numerically. It has been already corroborated that a Euler method (forward Euler) is reliable to solve this system provided the time step Δt is small enough¹⁴. We work with a lattice of distance Δx between the points, which is constant along the system and equal for each dimension (x, y, z). The scales chosen for the implementation were $\Delta x = 1$ for space and $\Delta t = 3 \cdot 10^{-4}$ for time.

Thus, we define the initial conditions of the order parameter $\phi(x, y, z)$ and compute the temporal evolution of the dynamic eq. (7). We should point out that there is complication when computing the contribution

$$\frac{12\phi}{1-\phi^2} T_1 + \frac{2(3\phi^2+1)}{(1-\phi^2)^2} T_2, \quad (8)$$

as in the bulk $(1-\phi^2) \rightarrow 0$ and this would diverge. We avoid this by adding a very small imaginary contribution to ϕ and implementing the integration using the residue theorem over the upper complex plane for equation (8).

In the dynamical equation (7), the bending and the Gaussian contributions can be differentiated by their energy moduli κ and κ_G , respectively. Thus, the Lagrange multiplier for the volume is not necessary since the dynamic equation is written

conservatively following the diffusion equation³⁹ (also known as model B). On the other hand, the Lagrange multiplier for the area conservation γ_A , that is necessary when working with finite closed membranes, will not be computed and considered as a constant, because we work with a reservoir for the surface area and the volume.

Thermal fluctuations

The thermal agitation of the membrane is modelled by white noise. This white noise represents the displacement generated by the random impacts of molecules on the membrane due to their random Brownian motion. Those impacts displace constantly the membrane from its average position moving different points of the membrane to different directions with various displacements. Therefore, we consider that thermal fluctuations are delta-correlated thorough space and time. This means that when one compares two different points of space, the fluctuations over a long enough time require to have no correlation between them, therefore being independent. It is necessary to have a noise that its intensity independent of time and space. From the Fluctuation Dissipation theorem, we can obtain the relation between the noise variance and the temperature via its auto-correlation which, for a noise ξ , takes the form

$$\langle \xi(\mathbf{x}, t) \xi(\mathbf{x}', t') \rangle = \frac{2k_B T}{\bar{\kappa}} \delta(\mathbf{x} - \mathbf{x}') \delta(t - t'), \quad (9)$$

where k_B is the Boltzmann constant and T the temperature. Its inverse dependence on the bending modulus κ comes from the fact that a higher rigidity reduces the thermal fluctuations of a membrane. This noise will be acting on the membrane position through the order parameter ϕ . The white noise has a mean $\langle \xi \rangle = 0$, a standard deviation σ and Gaussian probability distribution. The variance is the second moment of a single random variable ξ is defined by $\sigma^2 \equiv \langle [\xi - \langle \xi \rangle]^2 \rangle$ and is the measure of how much the values of ξ deviate from the mean value $\langle \xi \rangle$ ⁴⁰. The intensity of the noise can be measured with the variance σ^2 and from the Fluctuation Dissipation theorem, we know that for a thermal noise this variance is proportional to the temperature by

$$\sigma^2 = \frac{2k_B T}{\bar{\kappa}}. \quad (10)$$

We can identify in equation (9) that the magnitude of the auto-correlation is the variance σ^2 which can be modulated with a Gaussian distribution.

Now, to add this delta-correlated noise into the system, we consider that the membrane is obtained for the points in space defined by $\phi = 0$ and the interface relaxes fast to the hyperbolic tangent profile. Thereby, one can simply add a noise to the ϕ value around the points of the diffuse interface where $-1 < \phi < 1$. This would be written like

$$\frac{\partial \phi(\mathbf{x}, t)}{\partial t} = \nabla^2 \left(\frac{\delta F_{C_0}}{\delta \phi} + \frac{\delta F_K}{\delta \phi} \right) + \xi(\mathbf{x}, t)(1-\phi^2)/\varepsilon^2, \quad (11)$$

where the noise disturbs only the membrane while most of the bulk remains undisturbed.

Nonetheless, the noise has a Gaussian distribution with a mean zero, the conservation of volume and area can be violated. Even if the mean of the noise is zero for short time-scales we can find that the overall contribution of the noise is non-zero. Thus, one has to be careful when introducing temperature to a membrane system to ensure that the area and volume are conserved. Thus, to facilitate fission, we study a flat membrane with a reservoir of surface area and volume. It is known that individual closed vesicles should not be able to change area and volume⁴¹. This is more difficult to ensure for individual vesicles than it would be for the system as a whole. The vesicles size depend on the spontaneous curvature of the membrane⁴² in most cases the resulting vesicles are small¹⁰ and thus the membrane fluctuations cannot be taken as small for their length-scale. With their sizes the area and volume of the vesicles slightly change and fluctuate over time. This could be addressed by adding complex Lagrange multipliers to the model, however with the model as is one can study whether vesiculation happens or not, its energy, and the dynamics that bring a membrane to vesiculate. The proper modelling of the vesicles after they have scissioned from the mother membrane would add little or nothing given our goals.

The relaxation rate, and thus the spectrum, of membrane phase field models has already been studied on⁴³. There the authors found that the power spectrum falls with the wvector q as $\langle |h_q|^2 \rangle \propto q^{-5}$ where h_q is the deformation of the membrane in the Fourier space. The expected $\langle |h_q|^2 \rangle \propto q^{-4}$ is recovered when coupling the membrane to the Navier-Stokes equations⁴³. In the present model we do not introduce the Navier-Stokes equation. Here we want to study whether vesiculation happens or not, and under which conditions of energy modulus and temperature. The presented model thus should not be used to study the actual dynamics in real time without the addition of the hydrodynamic contribution. Our model in eq (4) is taking into account that the system is fluid and that the relaxation from a perturbation requires a conserved order parameter³⁸ giving a diffusion equation. It is known that in the case of phase transition dynamics when you use a diffusive dynamic equation you get an extra q^{-1} contribution on the power spectrum^{44,45}. The introduction of hydrodynamics cancels this contribution giving a $\langle |h_q|^2 \rangle \propto q^{-4}$ due to the Oseen tensor⁴³.

This does not invalidate any of the results we show. The drawback of this method is that we cannot study space-correlations without the complete model (including hydrodynamics). Moreover, we expect that the behaviour of the membrane when uncoupled with the fluid will be accurate for the low- q regime, which is the regime of big deformations and as such of vesiculation. Our current model will have less fluctuations in the high- q regime, and we expect the membrane to have less ripples and small deformations than an actual membrane.

3 Results

Negative Gaussian modulus

We focus on simulating flat infinite membranes where, as discussed earlier, there is an energy barrier that needs to be overcome to reach fission. With the white noise on the membrane position, we can mimic the effects of temperature. Thus, with

enough thermal energy, we expect the membrane to produce fission. However, this depends on the interplay between temperature and the bending and Gaussian rigidities κ and κ_G , respectively. That means that, if the temperature is not large enough, for a given κ and κ_G , one finds that even if the membrane can fluctuate, the fluctuations will not be enough to bend the membrane enough to produce a bud.

In the left side of Figure 1, we show a simulation with no noise at temperature $T = 0$. The membrane remains flat and no deformation occurs no matter how long the simulation runs. When one adds temperature to the flat membrane, one could start to see fluctuations that take the shape of something like the right side of Figure 1. In this case, the thermal fluctuations are not big enough to produce vesicle formation and one can define this as the fluctuating regime.

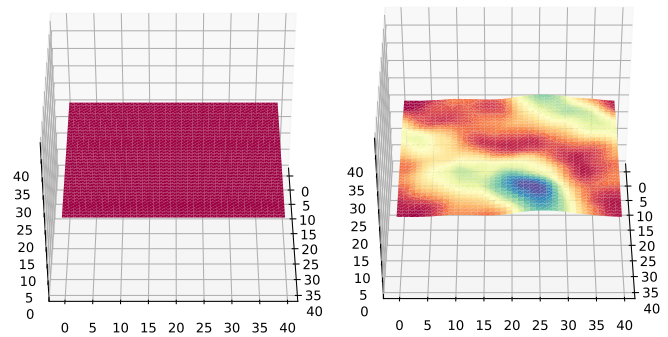


Fig. 1 **Left:** Snapshot of a flat membrane under conditions where fission is energetically favourable. However due to the starting geometry, we see no change over time on the membrane shape. The parameters used are $T = 0$, $\varepsilon = 1$, $\kappa = 1$, $\kappa_G = -10$ and $C_0 = -0.5$. **Right:** Snapshot of a fluctuating flat membrane under conditions where fission is energetically favourable and with low temperature. The parameters used are $T = 1.33 \cdot 10^{-5}$ in internal units (IU) defined in the text, $\varepsilon = 1$, $\kappa = 1$, $\kappa_G = -2$ and $C_0 = -0.25$. The color map of the membrane represent its local height. Red color means the membrane goes down and blue color means the membrane goes up.

With high enough temperature, we change into the vesiculation phase, where we can obtain vesicles from a flat membrane like in Figure 2. If we keep the simulation running, we can see vesicles keep forming until they fill up all the simulated space. Although the simulated vesicles after detachment do not conserve area nor volume perfectly the phenomenology of this system is all contained by the presented model for this kind of geometry. It has been proven that even a membrane with a geometry unfavourable for fission, if it is combined with temperature, one can obtain fission and vesicle formation.

Vesiculation phase diagram

The only remaining question is how the phase space for vesicle formation and fluctuating looks as a function of the free parameters. For that, we analyse the parameters that play an crucial role in whether fission happens or not. From the eq. (3) one sees that the free parameters are: T , κ_G/κ , and C_0 . Let us not forget that the real spontaneous curvature is slightly bigger than C_0 by $c_0 = \sqrt{2}C_0$.

In Figure 3, we obtain a phase diagram for fixed spontaneous

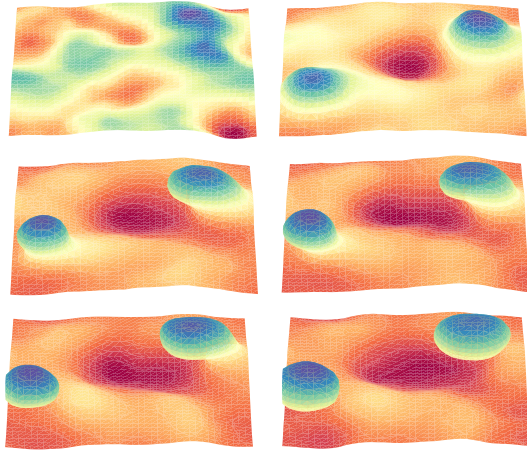


Fig. 2 Snapshots of a simulation where the membrane generates vesicles. From a flat membrane the system generates two vesicles from the oscillations produced by the temperature. The parameters used $T = 3.6 \cdot 10^{-5} (IU)$, $\varepsilon = 1$, $\kappa = 1$, $\kappa_G = -2$ and $C_0 = -0.25$. The color map of the membranes is present to aid height visualization. Red color means the membrane goes down and blue color means the membrane goes up.

curvatures $C_0 = -0.25$ and $C_0 = -0.10$. For low temperatures and low ratio $|\kappa_G/\kappa|$, we conserve fluctuation regime. On the contrary, when any of these quantities increases, we obtain vesicle formation. The spontaneous curvature value helps the vesiculation process. The bigger C_0 the bigger the drop in energy between a flat surface (with curvature zero) and the a spherical vesicle of literally any curvature value, as it will reduce the bending energy contribution $\kappa(C - C_0)^2$. We can see when comparing the two plots in Figure 3 that when decreasing the spontaneous curvature to $C_0 = -0.10$, there are areas in the phase diagram that change phase. It is be more pronounced for lower energy moduli ratios of κ_G/κ . However, one notes that the changes in C_0 generate qualitatively equal diagrams. Therefore, one can fix spontaneous curvature C_0 and explore only a phase diagram for the temperature T and the ratio $|\kappa_G/\kappa|$. Here we are only studying if the system vesiculates at very long times. Thus there will be no mixed-states.

In a deep analysis, the results in Figure 3 show that there is an energy barrier that one has to surpass to obtain vesicle formation. This energy barrier is being surpassed with the temperature. For any combination of C_0 and $|\kappa_G/\kappa|$ there is an energy barrier of a given magnitude, which decreases when increasing either C_0 or $|\kappa_G/\kappa|$. Thus, for a given energy barrier, as it is shown in the phase diagrams of the Figure 3, one sees how a minimum temperature is needed to be able to pass from the fluctuating phase into the vesiculating phase. Also, it is easy to see that from a given κ_G on-wards vesiculation happens for extremely low temperatures. This happens as the value of κ_G gets closer and surpasses the condition for spontaneous vesicle generation $-\bar{\kappa}_G > 2\bar{\kappa}$. Thus, the region where one sees a transition between fluctuating and vesiculating lies in the values $-\bar{\kappa}_G < 2\bar{\kappa}$, when increasing T and where the Gaussian modulus

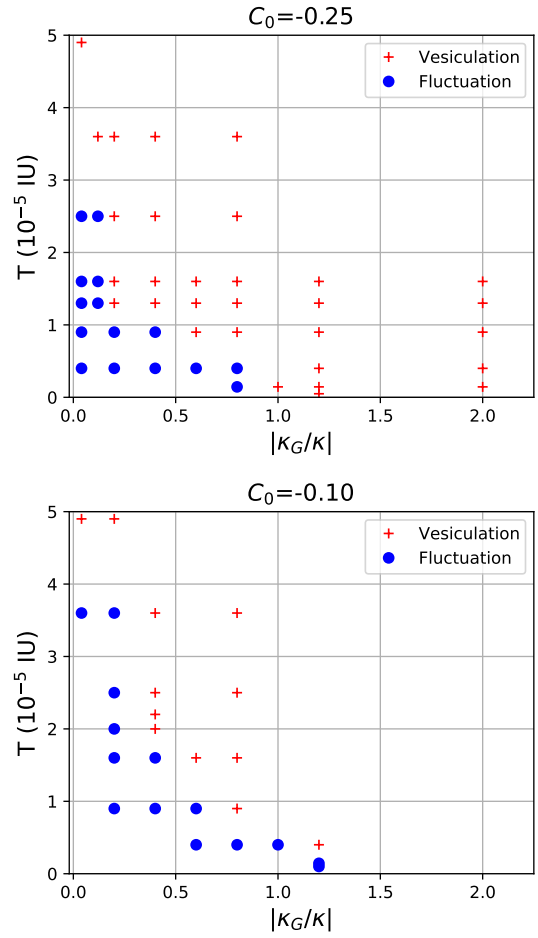


Fig. 3 Phase diagram of vesicle formation from a flat membrane depending on temperature T and the energy moduli ratio κ_G/κ for a fixed spontaneous curvature C_0 . The simulations had a size of $40 \times 40 \times 44$ and a membrane width of $\varepsilon = 1$.

is not big enough to fulfil spontaneous vesiculation. Otherwise, we find that if $k_B T$ is lower than the energy barrier, we shall not find vesiculation. Therefore, a system with a given temperature, the phase transition between spontaneous vesiculation and stable topology is displaced. This displacement is proportional to $k_B T$ and can be represented by a displacement of the phase transition. In Figure 4, we show the phase diagram for $\bar{\kappa}_G$ and $\bar{\kappa}$ modulus, respectively. The distance to the transition like $-\bar{\kappa}_G > 2\bar{\kappa}$ can be interpreted as an energy barrier. The farther away a system is from the line the higher the barrier there is. Therefore, the higher the temperature is needed to make that point in the phase space transition to the vesiculation regime.

Estimating the real temperature

For the estimation of the temperature, we will be using the Mean Square Displacement (MSD) $\langle |h|^2 \rangle$. To this end, we need to compute the exact position of the membrane over time. We do this by interpolating the position $\phi(x, y) = 0$ to obtain $h(x, y)$. For a flat membrane is easy as we only need to go through the direction z until finding the ϕ value closest to zero for each position

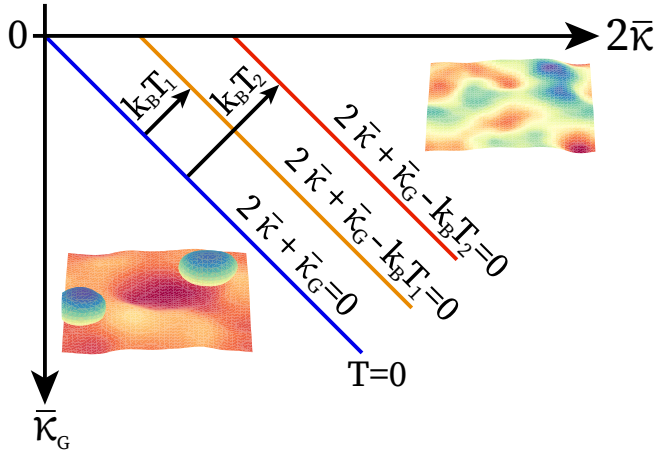


Fig. 4 Sketch of how the transition on the $\bar{\kappa}$ $\bar{\kappa}_G$ phase space moves with the thermal energy. Here we are using the original moduli $\bar{\kappa}$ and $\bar{\kappa}_G$ which have units of energy instead of the internal expressions used in the phase field model. The blue line corresponds to the condition $-\bar{\kappa}_G > 2\bar{\kappa}$ which is the case of eq (3) for $T = 0$. The other lines correspond to increasing temperature where $0 < T_1 < T_2$.

(x, y) . This value z will be our height $h(x, y) = z(x, y)$. With this information, we can use the following equation⁴⁶

$$\langle |h|^2 \rangle = \frac{k_B T}{2\pi \bar{\kappa}} q_{min}^{-2} = \frac{A k_B T}{8\pi^3 \bar{\kappa}}, \quad (12)$$

where $A = L^2$ is the surface area of the system we are simulating, L its length, and q_{min} is the lower cutoff wave-vector and has a value $q_{min} = 2\pi/\sqrt{A}$.

Using this expressions, we can compare the numerically obtained $\langle |h|^2 \rangle$ with the temperature T and the bending modulus $\bar{\kappa}$. We can easily know A and $\langle |h|^2 \rangle$ from a simulation and we can also fix $\bar{\kappa}$. Therefore, we can find the thermal energy of the system, from eq. (12), is

$$k_B T = 8\pi^3 \bar{\kappa} \frac{\langle |h|^2 \rangle}{A}, \quad (13)$$

and it is independent on the scale that we are simulating. Here, the relevant value is the ratio between the surface area and the MSD. Moreover, the final temperature depends strongly on the rigidity $\bar{\kappa}$. The bending modulus can take a wide range of values, from $\bar{\kappa} \approx 10k_B T_a$ to $\bar{\kappa} \approx 100k_B T_a$ where $T_a = 298K$. From this expression we can see that for a membrane with double the bending modulus $\bar{\kappa}$ we will need double the temperature to have the same MSD.

In the simulations, we are using internal computational units (IU). In the case of temperature these internal units are $\bar{\kappa}/k_B$, the question is now which is the value in Kelvins. To do this we use the mean square displacement of a number of simulations. The results of $\langle |h|^2 \rangle (\Delta x^2)$ for the average of various simulations can be seen in Table 1. Here, we can see that the mean square displacement $\langle |h|^2 \rangle (\Delta x^2)$ and the internal temperature T are following eq. (13) as the ratio of increase in T is followed by the MSD. With these, we can compare the thermal energy with the

T (IU)	$\langle h ^2 \rangle (\Delta x^2)$
$0.1 \cdot 10^{-5}$	0.008
$0.4 \cdot 10^{-5}$	0.030
$0.9 \cdot 10^{-5}$	0.075

Table 1 Mean square displacements $\langle |h|^2 \rangle$ obtained for different temperatures. The results of $\langle |h|^2 \rangle$ are taken from the average of three different simulations at the same temperature.

MSD. Introducing the MSD for $T = 0.9 \cdot 10^{-5}IU$ in eq. (13), one obtains $k_B T \approx 0.012\bar{\kappa}$.

We note that the final simulated temperature depends on the bending modulus of what we will be simulating. Using the ambient or room temperature $T_a = 293K$, the bending modulus for soft vesicles made of a lipid like DOPC, is $\bar{\kappa}_{DOPC} = 15k_B T_a$ ⁴⁷, for vesicles or more rigid red blood cells, $\bar{\kappa}_{RBC} = 70k_B T_a$, and for diseased or drugged red blood cells it can go even higher to $\bar{\kappa}_{RBCd} = 120k_B T_a$ ⁴⁸. Thus, the resulting thermal energy for each $\bar{\kappa}_{DOPC}$ and $\bar{\kappa}_{RBC}$ are $k_B T \approx 0.18k_B T_a$ and $k_B T \approx 0.84k_B T_a$, respectively. Therefore, depending on the bending modulus of the membrane $\bar{\kappa}$ at $T_{internal} = 0.9 \cdot 10^{-5}IU$, we are simulating around $T = 54K$ and $T = 250K$. This is a wide range of temperatures available to simulate. The results presented here range mainly from $T_{internal} = 0.1 \cdot 10^{-5}IU$ up to $T_{internal} = 3.6 \cdot 10^{-5}IU$, which result in the wide temperature ranges represented in Table 2. Observe that our results do not seem to represent adequate temperature ranges for soft membranes, like the DOPC. Thus our simulations can be used to represent a range of real biological membranes of high bending rigidity $\bar{\kappa}$ with realistic temperatures. To study what happens to softer membranes, one would have to simply simulate higher temperatures that match the biological range of a given bending modulus $\bar{\kappa}$.

Using Table 2, we can plot the region where water is in the liquid state in the previous phase diagram. In Figure 5, we show the dependency of the bending modulus in different regions of the phase diagram. With this, we can look for a given bending if a transition to vesiculation or fluctuation regimes is possible by changing T , C_0 , or $\bar{\kappa}_G$.

The length scales Δx and time scale Δt have to be compared to large membrane systems. For example formation of GUVs, deformation on large lipid bilayers surfaces, and other large membranes which takes a physical scale of around 1-10 μm . In these systems the time-scale of deformations will be in the magnitude of 10s. By comparison we can give a rough approximation of $\Delta x \sim 1\mu m$ and $\Delta t \sim 10^{-2}s$. So here we are talking about systems of size around $40 \times 40\mu m$. Looking at our computed C_0 the resulting vesicles in our simulations would be around $R_0 \sim 5\mu m$ for the results of Figure 5.

If we compare our results with DOPC systems, for example, which has a rather large spontaneous curvature of around $C_0 \approx 0.1/nm$ ⁴⁹. In these cases the resulting vesicles generated by spontaneous vesiculation would have a size around $R_0 \sim 10nm$. However, our results have to be compared to large systems as systems of nanometric length-scales require to take into account the monolayers themselves. For such scales one should use molecular dynamics or other microscopic approaches.

T (IU)	$0.9 \cdot 10^{-5}$	$1.6 \cdot 10^{-5}$	$3.6 \cdot 10^{-5}$
$\kappa = 15k_B T_a$	54 K	96 K	216 K
$\kappa = 30k_B T_a$	108 K	192 K	432 K
$\kappa = 70k_B T_a$	250 K	444 K	1000 K
$\kappa = 120k_B T_a$	460 K	850 K	1850 K

Table 2 Temperatures from IU to Kelvin for different internal values and different rigidities measured in $k_B T_a$ where $T_a = 298\text{K}$ and k_B is the Boltzmann constant.

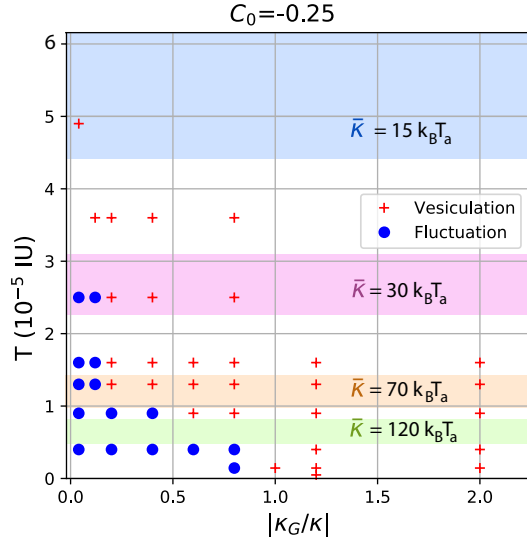


Fig. 5 Phase diagram of vesicle formation depending on temperature T and the energy moduli ratio $\bar{\kappa}_G/\bar{\kappa}$ for a fixed spontaneous curvature C_0 . In colours we find different regions where water is liquid depending on the bending modulus $\bar{\kappa}$. Simulations size of $40 \times 40 \times 44$ and membrane width $\varepsilon = 1$.

Energy evolution

We study the time evolution of both the Gaussian and the curvature energy contributions, represented in Figure 6. Here, one can see how for simulations where there is no vesiculation the energy curves remain flat over time, while for vesiculating systems the energy contributions decrease. However, looking at values that both terms take, we can see how the relative change in the Gaussian contribution is much greater than the one for the energy Curvature term F_{C_0} . Therefore, when a system is at the vesiculating phase, the dynamics of the system are driven mainly through the decrease in the Gaussian energy term F_K (see eq. (6)). This energy term starts decreasing once the first vesicles fission from the main membrane, but as there is an energy barrier to surpass, the simulations that do not have a high enough temperature cannot get to lower their Gaussian energy term.

In Figure 6, we obtain the curvature energy density F_{C_0}/A by using eq. (5) and the surface area of the membrane. This term in general decreases or remains constant, depending on whether we have vesicle formation or not. In simulations where we have a normal vesiculation process, the vesicles formed get a curvature closer to C_0 than when they were flat ($C = 0$) and thus reduce the term $(C - C_0)^2$ from the free energy. Our interest to study the

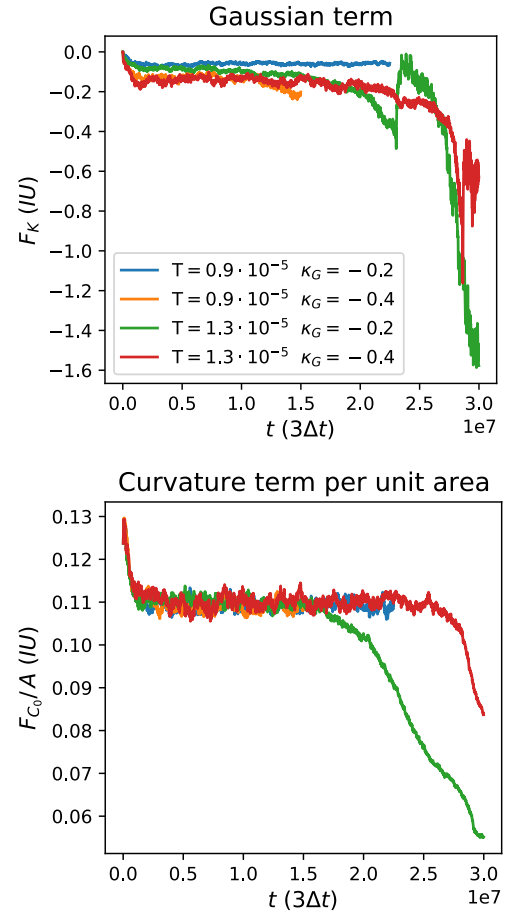


Fig. 6 Evolution over time of the two energy contributions for a series of simulations, in some there is vesiculation and in some there is not. From the bending free energy we have the Gaussian energy term F_K and the Curvature term energy density F_{C_0}/A . The curves that remained flat (blue and orange) remain on the fluctuating phase while the curves that decrease greatly (green and red) transition to the vesiculation phase. The energy is measured in $IU = \bar{\kappa}$ and the energy per unit area in $IU = \bar{\kappa}/\Delta x^2$

energy density of the curvature term instead of the total energy term is because as the surface area of the membrane increases over time the curvature energy contribution will also increase over time. This happens because in the end one has an energy cost in the curvature term of the free energy. Thus, any increase in surface area increases the curvature term of the free energy. Meanwhile, the Gaussian energy term, due to the Gauss-Bonnet theorem, is proportional to the number of objects and holes. In conclusion the best way to understand the evolution of the membrane in a vesiculation scenario where area is not conserved is to plot the complete Gaussian term and the Curvature term per unit area.

Finally, we study the chemical potential term squared $\int \mu^2 dV$, where the chemical potential is defined with the functional derivative $\mu = \delta F_{C_0}/\delta \phi$. This term shows the rate of change in the membrane. Looking at μ^2 , in Figure 7, we observe that there is a flat plateau when the membrane is in the fluctuating state. The value of this plateau is clearly related to the temperature of

the system, as all simulations at the same temperature overlap their plateaus. In cases where there will be vesiculation, this term starts climbing up as now there is an additional contribution to deformation other than temperature.

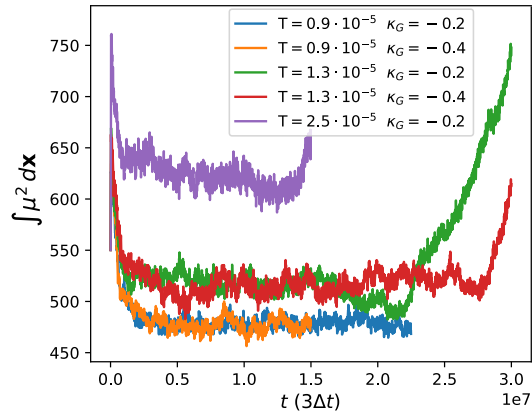


Fig. 7 Evolution over time of the chemical potential squared or μ^2 for different simulations. In the plot there are both simulations where vesiculation occurs and some simulations where it does not. Curves correspond to the same simulations as in Figure 6 with the addition of the purple curve.

Different values of κ_G will make so that the energy contribution of each vesicle created is bigger with increasing $|\kappa_G|$. This changes the rate of change over time for the Gaussian energy contribution. Thus the slope of the Gaussian energy term over time will depend on both temperature T and the Gaussian modulus κ_G . However, in Figure 8, one can see how by doubling the value of κ_G from the blue curve to the green one the slope of the Gaussian energy curve increases drastically, even with a lower T . Thus in this figure, one can see that the rate of change over time of the energy is very dependent on the Gaussian modulus κ_G . The temperature can be seen to change also that rate between the two simulations of Figure 8 that share the same modulus $\kappa_G = -1.2$. However, κ_G is more influential on the energy terms than the temperature.

For the curvature energy density in Figure 8, we can see a similar behaviour as in previous plots for most values of κ_G . However, in some cases the curvature term climbs back again. In these cases the κ_G is so big that its dominating over the curvature term and the vesicles deform in non-spherical ways to try to fit more vesicles at the cost of increasing the curvature energy term. Also, one can see how after a long time of vesiculation the Gaussian and Curvature energy terms stop changing and flattens again. This happens because in these simulations that have been left to run a long time the system reaches a point where all the space is full of vesicles and there is no room to produce any more.

Positive Gaussian modulus

Changing the sign of Gaussian modulus κ_G to a positive, one completely changes the results. Getting the system to transition from the fluctuating regime seems impossible, even for unrealistically high noise, the Gaussian contribution can hold the membrane together. The morphology of the membrane also changes,

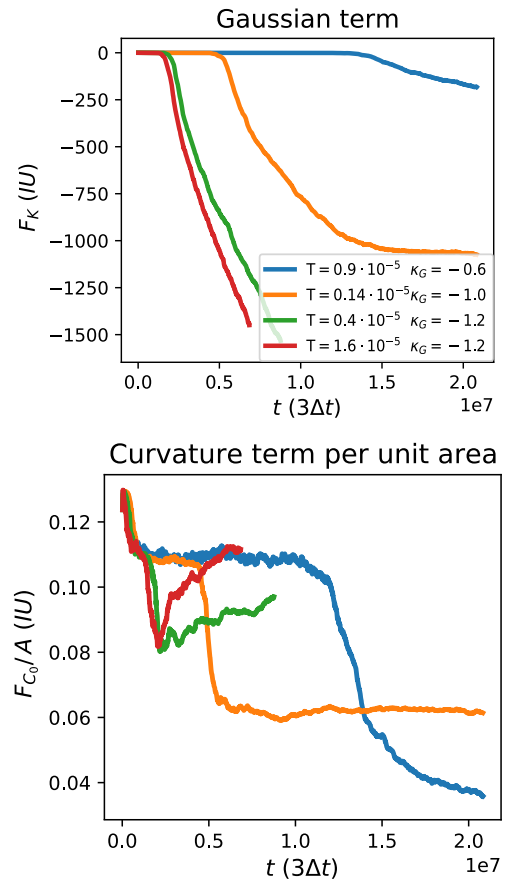


Fig. 8 Evolution over time of the two energy contributions for a series of simulations. From the bending free energy we have the Gaussian energy term and the Curvature term. In all simulations there is vesiculation and the main change in the rate at which the energy changes is mediated by the Gaussian modulus κ_G .

for very big noises like in Figure 9. We observe huge deformations and valleys much bigger than the size of the vesicles produced with negative κ_G . As high as these deformations are and as high as the temperature, the simulation never shows fission or handles.

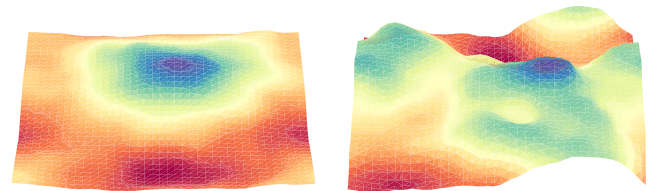


Fig. 9 Left: Membrane fluctuating with $T=6.4 \cdot 10^{-5}IU$, $\kappa_G = 0.4$, and $C_0 = -0.25$. **Right:** Membrane fluctuating with $T=256 \cdot 10^{-5}IU$, $\kappa_G = 0.4$, and $C_0 = -0.25$. Little matters the intensity of the noise, for positive Gaussian modulus we find no topological transitions. For very high noises the membrane curves and stays curved, but does not go further than that.

Some of the temperatures introduced in Figure 9 are two orders of magnitude over the previously simulated temperatures. Nonetheless, it seems to not matter how much thermal energy

we introduce the topology of the simulation never changes. The Gaussian term seems to be holding the membrane together, as for simulations with $\kappa_G = 0$ at these extremely high temperatures the system breaks down. Usually the Gaussian contribution is thought of only influencing the system when small membrane necks and other shapes close to topological transitions happen. However, the results obtained seem to suggest that the Gaussian term is changing radically how the membrane deforms at all stages and membrane geometries, at least for thermal fluctuations.

The lack of vesiculation makes sense given the Gauss-Bonnet theorem, when κ_G is taken positive, predicts that increasing the number of holes is what would lower the energy of the system. This however, does not happen. Even if the configuration is hard to achieve, the high temperatures used should be giving the necessary energy to produce any membrane deformation necessary. Therefore, maybe the most intriguing of all is not reaching a self-connected membrane like we see in a previous work¹⁴. One would expect with this level of noise to go through topological transitions but in the direction of increasing the number of holes and that decreasing the Euler characteristic and the Gaussian contribution. Thus, it seems that a flat membrane geometry is more difficult to generate holes and passages than to produce vesicles.

Turning off the temperature

The temperature is necessary to start the fission process. However, there is no need to maintain it after a certain time. Even for simulations where there has still not been a single fission event, if the membrane is already curved enough due to the temperature, even after turning off the noise it will end in multiple fission events.

Another consequence of the noise is that the vesicle shape and dynamics are slightly rough. One can see edges that one would not expect under normal circumstances as the resulting vesicles sometimes deform into rough shapes. This can be seen in the left plot of Figure 10. This happens because the vesicles are rather small and when in comparison with the thermal fluctuations the latter are big enough to deform the vesicles a lot. As the fluctuations are rather big at the size scale of a vesicle, it also makes more difficult to conserve area and volume and, most importantly, to be dominated the bending. However as stated earlier, the point of these simulations is not to have a rigorous description of the vesicles after the fission but to study the process that leads to fission.

To prove that this weird behaviour after fission is due to the noise and not to problems in the computation or the model, we study what happens if we turn the noise off mid-way through a simulation. One can see that after an initial kickoff where the membrane starts to be deformed enough to generate vesicles, even after turning off the temperature one will still get vesiculation. We can see this case in Figure 10, where after reaching a point where the membrane starts to generate vesicles we turn off the temperature and the vesicles behave more properly and vesiculation continues. This happens because the fluctuations made the system reach a much better geometry to fission and until reaching the steady state more vesicles will be formed only

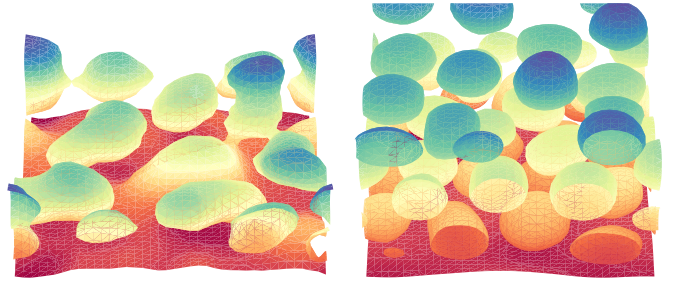


Fig. 10 Left: At very high T the membrane shape has more rough edges and might stick to new vesicles if there is no more room left. **Right:** Even after turning the noise off the initially flat membrane keeps generating vesicles, and the vesicles take their preferred spherical shape. This simulation was at $T = 144 \cdot 10^{-5}$ IU, $\kappa_G = -0.4$, and $C_0 = -0.25$.

due to the Gaussian energy contribution.

All this reflects the fact that temperature suffices to provide the system with enough energy to vesiculate.

4 Discussion

The conditions for spontaneous fission are present, a flat membrane will fission only in the presence of temperature, as one needs a trigger starting the process. Moreover, we see that through temperature, membranes that do not comply the original condition $-\bar{\kappa}_G > 2\bar{\kappa}$ can exhibit spontaneous fission. This is of great importance as membranes never are in a $T = 0$ scenario. In the end the thermal energy related to this noise by $E_T = k_B T$ is helping the system overcome an energy barrier ΔE to achieve vesiculation.

There are two possible states in the presence of temperature for the membrane: either its only fluctuating or its undergoing vesiculation. The phase diagrams show clearly how the spontaneous curvature C_0 , temperature T , and both Gaussian and bending moduli, κ_G and κ , influence in the transition. While C_0 changes the position of the transition in the diagram, it does not change the overall shape of the transition region. This transition is clearly seen in the region where the condition for spontaneous vesiculation $-\bar{\kappa}_G > 2\bar{\kappa}$ is not met and it happens because the region where the condition is met requires minimal temperature to trigger the vesiculation and the closer one is to meeting this condition the lower T is required for fission to start. The phase diagram (κ_G, κ) represented this displacement by changing the transition line as $\bar{\kappa}_G = -2\bar{\kappa} + k_B T$ (see Figure 4). The results clearly show how higher spontaneous curvatures help the vesiculation process by lowering the energy barrier ΔE to overcome.

For membranes with a positive Gaussian modulus κ_G , there is no temperature high enough so that it can transition from the fluctuating regime. We do not observe the membrane use the thermal fluctuations to create neither vesicles nor handles or passages as we see in¹⁴. One would expect with this level of noise to maybe go through topological transitions by increasing the number of holes. This points either to the flat geometry being bad to generate handles and passages or to the solution being unstable.

All the processes are driven mostly through the Gaussian en-

ergy term of the Helfrich free energy. This is seen in the relative change in the Gaussian energy term being greater than the energy term related to curvature as seen in Figure 6. The evolution of the Gaussian energy term seems to scale exponentially with the Gaussian rigidity κ_G while the influence of temperature T is much smaller (Figure 8). Also from a numerical point of view, there is value on working with the integral of the chemical potential squared $\int \mu^2 dx$, which clearly can be used to measure the temperature of the system.

These results can be exploited to measure the value of the Gaussian rigidity $\bar{\kappa}_G$ on real membranes. By introducing different proteins or substances that induce an spontaneous curvature C_0 and then exploring the whole available range of temperatures one should be able to find the transition from fluctuating to vesiculation. In the case that no transition is found, one could introduce a higher absolute value of C_0 and explore again all the available range of temperatures. The temperature at which the transition will end up happening will depend on the value of κ_G/κ . Given that the value of the bending modulus (or rigidity) κ is much easier to obtain experimentally than κ_G this could be a method for obtaining the Gaussian energy modulus.

An open question that remains is whether the different molecular machinery involved in some fission processes (e.g. the dynamic superfamily^{50–52} or the ESCRT machinery^{53,54}) work by lowering the observed energy barrier ΔE or simply produce fission regardless of ΔE . There is the possibility of this depending on the method that each molecular motor involved in fission uses. All these processes have a chemical rate and this rate is also dependent on temperature, so experiments on determining the nature on whether they are dependent on the energetic of the system or not could be challenging.

Acknowledgements

We acknowledge insightful discussions with F. Campelo, F. Monroy, J. Ignés-Mullol, I. Pagonabarraga, and R. Reigada. A.F.G. acknowledges financial support from MINECO (Spain) project FIS2016-78883-C2-1-P. Likewise, J.R.R.A. thanks the support from DAGAPA-UNAM grant IA-100823. A.H.M. acknowledges financial support from Ministerio de Ciencia e Innovación (MICINN, Spain) project PID2019-1060636B-100. J.R.R.A. and R.A.B. are grateful for the hospitality at the Universitat de Barcelona. R.A.B. was financially supported by Conacyt through project 283279.

Notes and references

- 1 J. E. Rothman and F. T. Wieland, *Science*, 1996, **272**, 227–234.
- 2 D. Njus, P. M. Kelley and G. J. Harnadek, *Biochimica et Biophysica Acta (BBA)-Reviews on Bioenergetics*, 1986, **853**, 237–265.
- 3 S. C. Silverstein, R. M. Steinman and Z. A. Cohn, *Annual review of biochemistry*, 1977, **46**, 669–722.
- 4 S. Miserey-Lenkei, G. Chalancon, S. Bardin, E. Formstecher, B. Goud and A. Echard, *Nature cell biology*, 2010, **12**, 645–654.
- 5 J. E. Rothman, *Nature*, 1994, **372**, 55–63.
- 6 G. Miesenböck, D. A. De Angelis and J. E. Rothman, *Nature*, 1998, **394**, 192–195.
- 7 N. S. Parkar, B. S. Akpa, L. C. Nitsche, L. E. Wedgewood, A. T. Place, M. S. Sverdlov, O. Chaga and R. D. Minshall, *Antioxidants & redox signaling*, 2009, **11**, 1301–1312.
- 8 S. Dharmavaram, S. B. She, G. Lázaro, M. F. Hagan and R. Bruinsma, *PLoS computational biology*, 2019, **15**, e1006602.
- 9 D. M. Eckert and P. S. Kim, *Annual review of biochemistry*, 2001, **70**, 777–810.
- 10 A. Alaarg, R. Schiffelers, W. W. van Solinge and R. Van Wijk, *Frontiers in physiology*, 2013, **4**, 365.
- 11 C. Has and S. Pan, *Journal of liposome research*, 2021, **31**, 90–111.
- 12 M. I. Angelova and D. S. Dimitrov, *Faraday discussions of the Chemical Society*, 1986, **81**, 303–311.
- 13 A. D. Bangham, M. M. Standish and J. C. Watkins, *Journal of molecular biology*, 1965, **13**, 238–IN27.
- 14 M. D. Rueda-Contreras, A. F. Gallen, J. R. Romero-Arias, A. Hernandez-Machado and R. A. Barrio, *Scientific Reports*, 2021, **11**, 1–10.
- 15 D. P. Siegel, *Biophysical journal*, 2008, **95**, 5200–5215.
- 16 R. E. Scott and P. B. Maercklein, *Journal of cell science*, 1979, **35**, 245–252.
- 17 L. Atia and S. Givli, *Journal of the Royal Society Interface*, 2014, **11**, 20131207.
- 18 R. Dimova, *Advances in colloid and interface science*, 2014, **208**, 225–234.
- 19 C. Has and P. Sunthar, *Journal of liposome research*, 2020, **30**, 336–365.
- 20 C. Leirer, B. Wunderlich, V. Myles and M. F. Schneider, *Biophysical chemistry*, 2009, **143**, 106–109.
- 21 N. L. Chanaday and E. T. Kavalali, *FEBS letters*, 2018, **592**, 3606–3614.
- 22 M. Laradji and P. S. Kumar, *Physical review letters*, 2004, **93**, 198105.
- 23 K. Yang and Y.-q. Ma, *The Journal of Physical Chemistry B*, 2009, **113**, 1048–1057.
- 24 K. Yang and Y.-q. Ma, *Soft Matter*, 2012, **8**, 606–618.
- 25 P. Bassereau, R. Jin, T. Baumgart, M. Deserno, R. Dimova, V. A. Frolov, P. V. Bashkurov, H. Grubmüller, R. Jahn, H. J. Risselada *et al.*, *Journal of physics D: Applied physics*, 2018, **51**, 343001.
- 26 F. Campelo and V. Malhotra, *Annual review of biochemistry*, 2012, **81**, 407–427.
- 27 M. P. Do Carmo, *Differential geometry of curves and surfaces: revised and updated second edition*, Courier Dover Publications, 2016.
- 28 D. P. Siegel and M. Kozlov, *Biophysical journal*, 2004, **87**, 366–374.
- 29 M. Hu, J. J. Briguglio and M. Deserno, *Biophysical journal*, 2012, **102**, 1403–1410.
- 30 H. Jung, B. Coldren, J. Zasadzinski, D. Iampietro and E. Kaler,

- Proceedings of the national academy of sciences*, 2001, **98**, 1353–1357.
- 31 F. Campelo, J. van Galen, G. Turacchio, S. Parashuraman, M. M. Kozlov, M. F. Garcia-Parajo and V. Malhotra, *Elife*, 2017, **6**, e24603.
 - 32 S. Morlot, V. Galli, M. Klein, N. Chiaruttini, J. Manzi, F. Humbert, L. Dinis, M. Lenz, G. Cappelletto and A. Roux, *Cell*, 2012, **151**, 619–629.
 - 33 F. Campelo and A. Hernández-Machado, *Physical Review Letters*, 2008, **100**, 158103.
 - 34 T. Biben, K. Kassner and C. Misbah, *Physical Review E*, 2005, **72**, 041921.
 - 35 G. R. Lázaro, A. Hernández-Machado and I. Pagonabarraga, *Soft Matter*, 2014, **10**, 7195–7206.
 - 36 Q. Du, C. Liu and X. Wang, *Journal of Computational Physics*, 2004, **198**, 450–468.
 - 37 F. Campelo and A. Hernandez-Machado, *The European Physical Journal E*, 2006, **20**, 37–45.
 - 38 P. C. Hohenberg and B. I. Halperin, *Reviews of Modern Physics*, 1977, **49**, 435.
 - 39 F. Campelo, *Shapes in cells. Dynamic instabilities, morphology, and curvature in biological membranes.*, Universitat de Barcelona, Spain, 2008.
 - 40 C. W. Gardiner *et al.*, *Handbook of stochastic methods*, Springer Berlin, 1985, vol. 3.
 - 41 W. Helfrich, *Zeitschrift für Naturforschung C*, 1973, **28**, 693–703.
 - 42 U. Seifert, K. Berndl and R. Lipowsky, *Physical Review A*, 1991, **44**, 1182.
 - 43 G. R. Lázaro, I. Pagonabarraga and A. Hernández-Machado, *The European Physical Journal E*, 2017, **40**, 77.
 - 44 J. D. Gunton and M. Droz, *Introduction to the theory of metastable and unstable states*, Springer, 1983.
 - 45 D. Jasnow and R. K. Zia, *Physical Review A*, 1987, **36**, 2243.
 - 46 H. Strey, M. Peterson and E. Sackmann, *Biophysical Journal*, 1995, **69**, 478–488.
 - 47 J. F. Nagle, M. S. Jablin, S. Tristram-Nagle and K. Akabori, *Chemistry and physics of lipids*, 2015, **185**, 3–10.
 - 48 R. Rodríguez-García, I. López-Montero, M. Mell, G. Egea, N. S. Gov and F. Monroy, *Biophysical Journal*, 2015, **108**, 2794–2806.
 - 49 B. Kollmitzer, P. Heftberger, M. Rappolt and G. Pabst, *Soft matter*, 2013, **9**, 10877–10884.
 - 50 S. L. Schmid and V. A. Frolov, *Annual review of cell and developmental biology*, 2011, **27**, 79–105.
 - 51 J. E. Hinshaw and S. L. Schmid, *Nature*, 1995, **374**, 190–192.
 - 52 S. M. Svezter and J. E. Hinshaw, *Cell*, 1998, **93**, 1021–1029.
 - 53 M. Bleck, M. S. Itano, D. S. Johnson, V. K. Thomas, A. J. North, P. D. Bieniasz and S. M. Simon, *Proceedings of the National Academy of Sciences*, 2014, **111**, 12211–12216.
 - 54 S. B. Van Engelenburg, G. Shtengel, P. Sengupta, K. Waki, M. Jarnik, S. D. Ablan, E. O. Freed, H. F. Hess and J. Lippincott-Schwartz, *Science*, 2014, **343**, 653–656.